Proceedings of the International Conference on Nuclear Shapes

THE VARIETY OF NUCLEAR SHAPES

Aghia Pelaghai, Crete, Greece
June 29 — July 3, 1987

Editors
J. D. Garrett
C. A. Kalfas
G. Anagnostatos
E. Kossionides
R. Vlastou

World Scientific
Singapore • New Jersey • Hong Kong

Effects of Static and Dynamical Triaxial Deformations on Properties of B(M1) and B(E2) in Odd-A, High-Spin States

M. MATSUZAKI, Y.R. SHIMIZU* and K. MATSUYANAGI

Department of Physics, Kyoto University, Kyoto 606, JAPAN
* Department of Physics, Kyushu University, Fukuoka 812, JAPAN

ABSTRACT

Effects of both the static and the dynamical triaxial deformations on the signature dependence of B(M1) and B(E2) in odd-A nuclei are studied by applying the RPA formalism based on the rotating (cranked) shell model to odd-A nuclei. Typical results of numerical calculation are presented for ^{165}Lu and ^{157}Ho, for which most detailed experimental data are available.

The main purpose of this talk is to discuss the effects of triaxial deformations on properties of B(M1) and B(E2) between high-spin, unique-parity states in odd-A nuclei. We shall consider both static and dynamical deformations away from axial symmetry. By "static triaxial deformations" we mean equilibrium shapes deviating from axial symmetry, while we call vibrations in the gamma degree of freedom (shape-fluctuations about the equilibrium point) "dynamical triaxial deformations."

As was pointed out by Hamamoto and Mottelson,[1),2)] occurrence of triaxial equilibrium shapes is expected to bring about a characteristic dependence of B(E2; $\Delta I=-1$) on the signature quantum number α of the high-spin, unique-parity states in odd-A nuclei. The signature α is, as is well known, related to the angular momentum I by $I=\alpha+\text{even}$. On the other hand, the B(M1; $\Delta I=-1$) are expected to exhibit a strong signature dependence already in the axial symmetric case, since they are closely related to the signature splittings of the quasiparticle energies which generally occur in the rotating frame. As a matter of fact, the B(M1) is also affected by the triaxial shapes, because the signature splittings depend on the triaxiality parameter γ_0 of the rotating potential.

In fact, strong signature dependences of B(M1) and B(E2) have been observed in the $\Delta I=-1$ transitions between high-spin, unique-parity states in odd-A nuclei.[3),4)] These recent experimental data have been discussed by Hamamoto and Mottelson[1),2)] mainly by means of the particle-rotor model.

The basic aim of our work is to develop, on the basis of the rotating (cranked) shell model, a microscopic description of odd-A high-spin states along the line parallel to the particle-rotor model. Our model may be regarded as a particular version of the particle-rotor model, because the basis of the intrinsic state vectors is determined by the rotating (cranked) shell model as a function of the rotational frequency ω_{rot}. Our model may also be regarded as an extension of the traditional quasiparticle-vibration coupling models, like the Kisslinger-Sorensen's one[5)] and the Soloviev's one,[6)] into the rotating frame of reference. One of the merits of our approach is that it can be easily applied to high-spin states involving many aligned quasiparticles, whereas in the conventional particle-rotor model the treatment of the multi-nucleon-aligned bands becomes increasingly difficult with increasing number of aligned nucleons. On the other hand, our model has a limitation that the gamma vibrations and the wobbling modes are treated by the RPA within the small amplitude approximation.

Our microscopic approach consists of the following four steps.

1) We construct a diabatic quasiparticle representation for a deformed potential which is uniformly rotating with angular frequency ω_{rot}. The single-particle potential is of the Nilsson plus BCS form and is axially asymmetric in general. This step provides us with a diabatic basis for the rotating (cranked) shell model. The diabatic basis enables us to unambiguously specify individual rotational bands in which internal structures of the quasiparticle state vectors

smoothly change as functions of ω_{rot}.

2) The residual interaction between quasiparticles consists of the monopole-pairing and the doubly-stretched quadrupole forces, and is treated by means of the RPA in the rotating frame. This step determines the normal modes of vibration.

3) For odd-A nuclei, the couplings between the aligned quasiparticles and the gamma vibrations in the rotating frame (see Fig.1) are treated in the same manner as in the traditional quasiparticle-phonon coupling models.[5),6)]

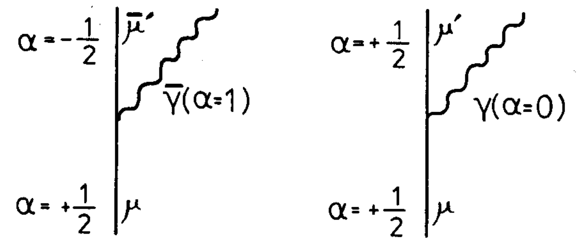

Fig.1 Elementary vertices of the couplings between the quasiparticles (solid lines) and the gamma vibrations (wavy lines). The signatures α of these modes are indicated.

The internal wave functions $|\chi_n(\omega_{rot})\rangle$ are then written as superpositions of the quasiparticle (a^+) and the gamma-vibrational (X^+) excitations :

$$|\chi_n(\omega_{rot})\rangle = \sum_\mu \psi_n^{(1)}(\mu)\, a_\mu^+ |\phi\rangle + \sum \psi_n^{(3)}(\mu\gamma)\, a_\mu^+ X_\gamma^+ |\phi\rangle + \sum \psi_n^{(3)}(\bar\mu\bar\gamma)\, a_{\bar\mu}^+ X_{\bar\gamma}^+ |\phi\rangle + \cdots, \quad (1)$$

where X_γ^+ and $X_{\bar\gamma}^+$ represent the gamma vibrations with positive (α=0) and negative (α=1) signatures, respectively. These internal wave functions are calculated for each value of ω_{rot}. The gamma vibrations are taken into account up to the two-phonon states.

4) We extend the Marshalek's treatment[7)] of the "Nambu-Goldstone modes", Γ^+ and Γ, in the RPA (which reorient the angular momentum

of the collective rotation) to odd-A nuclei. Namely, we make the following replacement

$$\Gamma^{+} = \frac{1}{\sqrt{2I_0}}(\hat{J}_-)_{RPA} \longrightarrow \frac{1}{\sqrt{2I_0}}(\hat{I}_- - \hat{J}_-^{(qp)}),$$
$$\Gamma = \frac{1}{\sqrt{2I_0}}(\hat{J}_+)_{RPA} \longrightarrow \frac{1}{\sqrt{2I_0}}(\hat{I}_+ - \hat{J}_+^{(qp)}), \tag{2}$$

where $(\hat{J}_\pm)_{RPA}$ denote the RPA approximations for the original (microscopic) angular momentum operators, and $\hat{I}_\pm$ and $\hat{J}_\pm^{(qp)}$ represent the total (external) and the quasiparticle (internal) angular momenta, respectively. This ansatz is the most crucial point of our approach, and corresponds to the fact that the state vectors are constructed in a direct product form of the rotational and the internal wave functions :

$$|\Psi_{nIMK}(\omega_{rot})\rangle = |IMK\rangle \otimes |\chi_n(\omega_{rot})\rangle . \tag{3}$$

We adopt the Holstein-Primakoff-type boson representation for the D-functions. Then, the rotational wave functions $|IMK\rangle$ can be written in the subspace K=I in the following form:[7]

$$|I I_0 I\rangle = \frac{1}{\sqrt{2\pi}} e^{i(I-I_0)\Phi} \frac{1}{\sqrt{(I-I_0)!}} (b^+)^{I-I_0} |I_0 I_0 I_0\rangle \tag{4}$$

where K is the projection on the x-axis which is identified with the rotation axis.

By means of the above procedure, we obtain microscopic expressions for the intrinsic M1 and E2 operators as follows :

M1 transitions with ΔI=-1

$$\hat{\mu}_{-1}^{(in)} = (g_\ell - g_{RPA})\hat{\ell}_{-1}^{(qp)} + (g_s^{(eff)} - g_{RPA})\hat{s}_{-1}^{(qp)} + \sum_n (\mu_n^{(-1)} X_n^+ + \mu_n^{(+1)} X_n), \tag{5}$$

where $\hat{l}^{(qp)}$ and $\hat{s}^{(qp)}$ denote the orbital and the spin angular momenta of quasiparticles. The effective g-factor of the RPA vacuum state, g_{RPA}, can be written as[1)]

$$g_{RPA} \equiv \frac{\langle \hat{\mu}_x \rangle}{\langle \hat{J}_x \rangle} = g_R + (g_i - g_R)\frac{i}{R+i}, \tag{6}$$

where i and R are the angular momenta produced by the aligned quasiparticles and the collective rotations, respectively, and g_R denotes the rotational g-factor. We see from the above expression that B(M1) values would increase when the $(\nu i_{13/2})^2$ alignment takes place, because g_{RPA} is reduced by this alignment effect.

E2 transitions with ΔI=-1

$$\frac{1}{i}\hat{Q}_{2-1}^{(in)} = -\sqrt{\frac{3}{2}}\langle Q_0\rangle \frac{\hat{J}_z^{(qp)}}{I_0} + \langle Q_2\rangle\left(2\frac{i\hat{J}_y^{(qp)}}{I_0} + \frac{\hat{J}_z^{(qp)}}{I_0}\right) + \sum_n (\Lambda_n^{(-1)} X_n^+ + \Lambda_n^{(+1)} X_n) + \frac{1}{i}\hat{Q}_{2-1}^{(qp)}$$
$$\approx \left\{ -\sqrt{\frac{3}{2}}\langle Q_0\rangle + \langle Q_2\rangle\left(1 + 2(-1)^{I-j}\left|\frac{\Delta E}{\hbar\omega_{rot}}\right|\right)\right\}\frac{\hat{J}_z^{(qp)}}{I_0} + \sum_n (\Lambda_n^{(-1)} X_n^+ + \Lambda_n^{(+1)} X_n), \tag{7}$$

where $\hat{Q}_{2-1}^{(in)}$ is quantized along the x-axis while $\langle Q_K\rangle$ (K=0,2) are along the z-axis. In Eq.(7), we have eliminated the operator $i\hat{J}_y^{(qp)}$ by using an approximate relation

$$i\hat{J}_y^{(qp)} \approx (-1)^{I-j}\left|\frac{\Delta E}{\hbar\omega_{rot}}\right| \hat{J}_z^{(qp)}, \tag{8}$$

which becomes exact in the axially symmetric limit. Here I is the angular momentum of the initial state, and ΔE denotes the signature splitting of the quasiparticle energies associated with the large-j, unique-parity orbit. We note that the phase factor $(-1)^{I-j}$ is positive (negative) for the favoured (unfavoured) states. This alternation in sign brings about a characteristic signature dependence of the B(E2; $\Delta I=-1$) when $\langle Q_2 \rangle \neq 0$. If the vibrational contributions are neglected, this expression reduces to that of Hamamoto[1] when j=1/2, because the factor $(-1)^{I-j}|\Delta E/\hbar\omega_{rot}|$ becomes $(-1)^{I-1/2}$ for j=1/2.

Below we present typical results of numerical calculations for ^{165}Lu and ^{157}Ho, for which most detailed experimental data are available. In these calculations, we use the same static triaxial deformation parameters as in Hamamoto and Mottelson,[1),2)] except for the five-quasiparticle aligned band of ^{165}Lu where $\gamma_0=0°$ is assumed. The procedure for fixing other parameters entering in the calculation is described in Ref.8).

Figure 2 shows the ratio B(M1; $I \to I-1$)/B(E2; $I \to I-2$) for ^{165}Lu as a function of ω_{rot}. The solid (broken) lines represent the ratios calculated by (without) taking into account the couplings with the gamma vibrations. The observed rotational bands may be roughly classified into three groups according to the number of aligned quasiparticles. The first group ($15/2 \lesssim I \lesssim 29/2$) involves the aligned quasiparticle A_p or B_p. The second ($35/2 \lesssim I \lesssim 51/2$) involves the quasiparticle configuration $A_pA_nB_n$ or $B_pA_nB_n$. The third ($I \gtrsim 59/2$) involves $A_pA_nB_nC_nD_n$ or $B_pA_nB_nC_nD_n$. Here, A_p, B_p and A_n,B_n, C_n, D_n are the familiar notations denoting the aligned quasiparticle states associated with the $\pi h_{11/2}$- and $\nu i_{13/2}$-orbits, respectively. Note that we obtain the crossing between the second and the third configurations at $\hbar\omega_{rot} \approx 0.4$ MeV in good agreement with the suggestion from the experiment.[3)] The interactions between the two configurations are neglected in our calculation with the use of the diabatic representation, although the experimental data indicate that these are rather strong. We have selfconsistently calculated the pairing gaps. The resulting neutron gap Δ_n is, for instance, 0.72

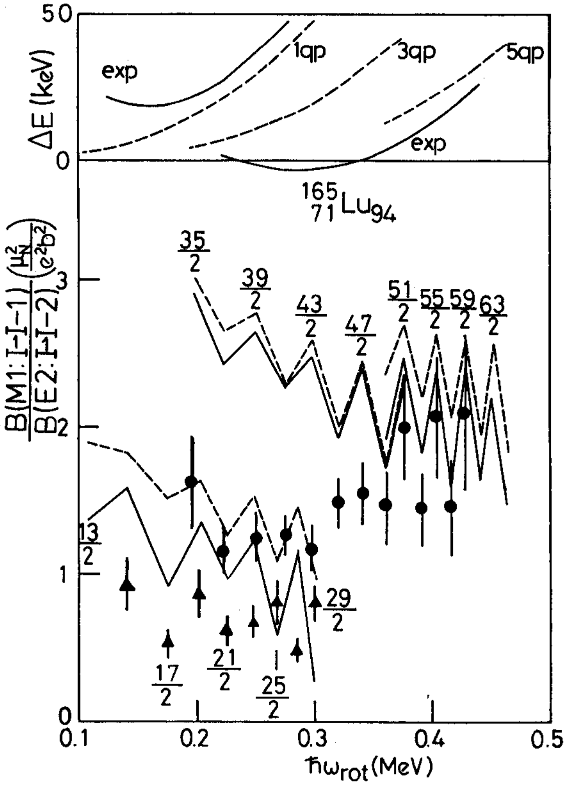

Fig.2 The ratios B(M1; $I \to I-1$)/B(E2; $I \to I-2$) plotted as a function of ω_{rot}. The solid triangles and the solid circles with error bars denote the experimental data. The solid (broken) lines represent the results of calculation with (without) taking into account the couplings with the gamma-vibrations. The triaxial deformation parameters are assumed to be γ_0 =18°,10° and 0° for the one, three and five quasiparticle bands, respectively. Note that our definition of the sign of γ_0 is opposite to the Lund convention. Other parameters of calculation are : β =0.21, $g_s^{(eff)}=0.7g_s^{(free)}$, Δ_p =1.18 MeV, Δ_n=1.16 MeV for the one-quasiparticle band, Δ_p =1.18 MeV, Δ_n =0.72 MeV for the three-quasiparticle band, and Δ_p =1.18 MeV, Δ_n=0 for the five-quasiparticle band. In the upper portion of this figure, calculated values for the signature-splittings of the quasiparticle energies are compared with the experimetnal ones.

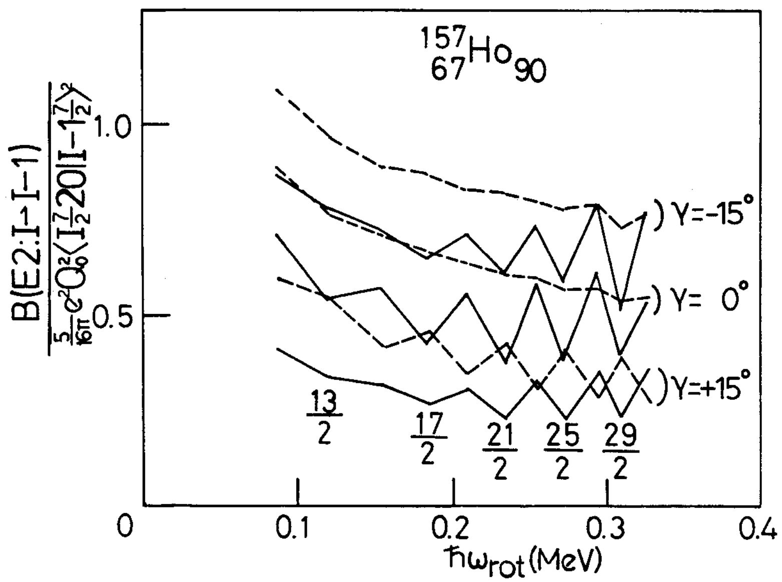

Fig.3 The calculated values of B(E2; I→I-1) divided by $(5/16\pi)\langle eQ_o\rangle^2\langle I,7/2,2,0|I-1,7/2\rangle^2$. The three cases with different γ_o values (γ_o=±15°,0°) are displayed. The solid (broken) lines show the results with (without) taking the couplings with the gamma-vibrations into account. The deformation parameters used are β=0.20, Δ_p=1.21 and Δ_n=1.25 MeV.

MeV at $\hbar\omega_{rot}$=0.2 MeV for the three-quasiparticle band and vanishes for the five-quasiparticle band. We see in this figure that the signature dependence is well reproduced especially in the highest-spin region. Another interesting feature of Fig.2 is that the ratio increases when the $i_{13/2}$ neutrons align. This trend is caused by the decrease of the g_{RPA}. The calculated values of g_{RPA} are 0.29∼0.27 for the one-quasiparticle band, -0.12∼-0.04 for the three-quasiparticle band, and -0.05∼0.04 for the five quasiparticle band. These values of g_{RPA} smoothly change as a function of ω_{rot} within individual bands. For the sake of reference, we mention that the static triaxial deformations (which we calculated by using the "isotropic velocity distribution condition"[8]) are γ_0=0°∼8° for the one-quasiparticle band, γ_0 = 6°∼11° for the three-quasiparticle band, and $\gamma_0 \approx 0°$ for the five quasiparticle band (Note that our definition of the sign of γ_0 is opposite to the Lund convention.[1]) These values of γ_0 smoothly change as a function of ω_{rot} within individual bands.

Figure 3 shows the calculated values of B(E2; I→I-1) for ^{157}Ho. It is seen that the signature dependence originating from the couplings with the gamma-vibrations is stronger than that from the static triaxial deformations. Consequently, the B(E2; I→I-1) from the favoured states (whose I=j+even) become always larger than those from the unfavoured states (whose I=j+odd), in agreement with the experimental data.[4] On the other hand, the calculated signature dependence of B(E2) is smaller in magnitude than experimental data. Also, the large experimental values[4] of the ratio B(E2; I→I-1)/B(E2; I→I-2) could not be reproduced. In this connection, we note that the calculated values of the factor $\Delta E/\hbar\omega_{rot}$ are 0.43, 0.08 and -0.05 for γ_0=15°, 0° and -15°, respectively, at $\hbar\omega_{rot}$=0.2 MeV in ^{157}Ho, which are considerably smaller than unity. Thus, the signature dependence originating from the static triaxial deformations is significantly suppressed in this nucleus.

We have carried out a systematic analysis also for other odd-A nuclei, and the results of calculation are available for further discussions.

1) I. Hamamoto, Proc. Niels Bohr Centennial Conf. on Nuclear Structure, Copenhagen 1985, ed. R. Broglia, G.B. Hagemann and B. Herskind (North-Holland, 1985), p.129, and references therein.
2) I. Hamamoto and B. Mottelson, Phys. Lett. 167B(1986), 370.
3) P. Frandsen et al., Phys. Lett. B177(1986), 287.
4) G.B. Hagemann et al., Nucl. Phys. A424(1984), 365.
5) L.S. Kisslinger and R.A. Sorensen, Rev. Mod. Phys. 35(1963), 853.
6) V.G. Soloviev, Theory of Complex Nuclei, Nauka, Moscow, 1971. (Transl. Pergamon Press, 1976)
7) E.R. Marshalek, Nucl. Phys. A275(1977), 416.
8) Y.R. Shimizu and K. Matsuyanagi, Prog. Theor. Phys. 70(1983) 144; 71(1984) 960; 72(1984) 799; 74(1985) 1346.